Carbohydrate Polymer Technologies and Applications 5 (2023) 100271

Contents lists available at ScienceDirect

Carbohydrate Polymer Technologies and Applications

journal homepage: www.sciencedirect.com/journal/carbohydrate-polymer-technologies-and-applications

# Diffusion of Thyme, Cinnamon and Oregano essential oils in different nanocellulose matrices

Sara Casalini, Federico Montanari, Marco Giacinti Baschetti *

*Department of Civil, Chemical, Environmental and Materials Engineering-DICAM, University of Bologna, via Terracini 28, 40131 Bologna BO, Italy*

ARTICLE INFO

*Keywords:*
Nanocellulose
Essential oil
Release kinetics
Diffusivity
Bio-Active packaging

ABSTRACT

Solubility and diffusivity of Thyme, Cinnamon and Oregano essential oils in nanocellulose films, with different carboxymethylation degree, were investigated in view of potential use in active packaging applications.

Solubility of liquid essential oils resulted to increase with the carboxymethylation degree for both Oregano and Thyme, while it was non-monotonous for Cinnamon. Thyme showed the higher solubility (about 20%wt) followed by Cinnamon and Oregano.

The sorption kinetics of liquid essential oils was substantially Fickian. The diffusivity also increased with the increase of the carboxymethylation degree, going from $9.6 \times 10^{-9}$ $cm^2/s$, observed for oregano in pure nanocellulose, to $2.0 \times 10^{-8}$ $cm^2/s$, measured for Cinnamon in the most charged one.

The release in vapor phase showed two different kinetics: a faster one dominating at short times and a slower one visible at long times. Fickian diffusion described the behaviour of most of the samples even if in some case data were better fitted by using exponential functions. In general, Diffusivities values ranged from $10^{-9}$ to $10^{-11}$ $cm^2/s$ for the fast process and from $10^{-11}$ to $10^{-13}$ $cm^2/s$, for the slow one.

Carboxymethylation degree also affected the release kinetics of antimicrobial essential oils, which therefore can be tuned by appropriate choice of the nanocellulose material.

## 1. Introduction

In the recent years, the need for a more sustainable lifestyle has become one of the main drivers in consumers choice. In the packaging field this fact has brought the attention to the development of new solutions based on biodegradable and bio-based materials to replace oil-based polymers (Agarwal, 2020; Zhao et al., 2020). In parallel, the research about active bio-based packaging has significantly increased in the last years (Wróblewska-Krepsztul et al., 2018) as it extends the concept of sustainable packaging by coupling the use of renewable materials with the shelf-life increase (Yildirim et al., 2018; Yousefi et al., 2019), thus reducing at the same time environmental impact and the food waste (Wikström et al., 2019). Therefore, a number of new composite materials have been investigated and coupled with different active agents, strengthening the idea of circular economy (Silvestre et al., 2011; Youssef & El-Sayed, 2018).

Among the different possibilities, nanocellulose is one of the most studied biopolymers for active packaging applications (Bras & Saini, 2017; Ferrer et al., 2017; Khan et al., 2014a; Li et al., 2015). It is the most abundant biopolymer on earth, and its biodegradability and nanoscale properties paved the way to many new applications making it one of the most studied biopolymers (Klemm et al., 2018). Nanocellulose is obtained directly from cellulose as nanofibrils (also called micro/-nanofibrillated cellulose) or nanocrystals, or it can be produced by bacteria through a biotechnological process (Nagarajan et al., 2021; Reshmy et al., 2021; Ibrahim et al., 2020). The raw material from which nanocellulose is obtained, the pre-treatment applied and the process itself can variate, conferring different properties to the final material (García et al., 2016; Khalil et al., 2014; Pradhan et al., 2022; Qing et al., 2013). Moreover, the possibility of applying various surface modifications, which act on the chemical structure, makes it very versatile (Habibi, 2014; Missoum et al., 2013; Rol et al., 2019). In fact, it has been largely used both as nanofiller and as matrix itself, by adapting its features to the requests of the particular application (Ansaloni et al., 2017; Chi & Catchmark, 2018; Shojaeiarani et al., 2021; Vilarinho et al., 2018).

The use of nanocellulose resulted very promising in the field of active packaging, where the advantages of the nanofibers effects can be

* Corresponding author.
*E-mail address:* marco.giacinti@unibo.it (M. Giacinti Baschetti).

https://doi.org/10.1016/j.carpta.2022.100271

Available online 8 December 2022

coupled with the extension of the shelf-life due to the antimicrobial properties of the active agents (Ahankari et al., 2021a). Regarding this specific application, natural antimicrobial agents have been favoured, in the last years, with respect to inorganic ones, due to their intrinsic sustainability (Azeredo et al., 2017; Othman, 2014). Among these, the essential oils (EOs) arouse certain attention, thanks to their well-known antimicrobial activity against a broad spectrum of food pathogens, their natural origin and safety (Khan et al., 2014b; Montero et al., 2021; Syafiq et al., 2021a).

EOs are volatile and aromatic oily liquids obtained from plants. They exhibit antimicrobial and antioxidant properties which made them interesting compounds to be included into food packaging formulations (Atarés & Chiralt, 2016; Burt, 2004; Hammer et al., 1999a). The most common plants from which they are derived are Rosemary, Oregano, Lemongrass, Thyme and others (Ribeiro-Santos, Andrade, de Melo, et al., 2017). The oils contain a mixture of various components which influence the antimicrobial activity and depend on the plant type, on the harvesting and growing conditions and the geographical area (Hammer et al., 1999b).

Many studies are available on the EOs' mechanical and antimicrobial effects on bio-based polymers, such as nanocellulose alone or coupled with other biopolymers (Atarés & Chiralt, 2016; Khaledian et al., 2019; Khan et al., 2014a). The main aim is to give to the composite material antimicrobial and antioxidant effects thanks to EOs properties, while not endangering the mechanical or barrier properties of the base materials (Dannenberg et al., 2017; Khaledian et al., 2019; Salmieri et al., 2014).

Currently, most of these studies utilize a very pragmatical approach, based on the production and testing of new composite materials in terms of mechanical, barrier and antimicrobial properties, by considering the effect on specific bacteria or on the shelf life of well-defined food (Casalini & Baschetti, 2022). There is, instead, a limited amount of works focusing on fundamental aspects, such as the study of the solution and diffusion properties, which, however, have a great importance on the final efficiency of the active packaging solution. In most application, indeed, EOs need to diffuse out from the active film to express their antimicrobial activity on the food products and in the headspace of the package (Ribeiro-Santos et al., 2017). An accurate control of the loading and of the release rate of antimicrobial agent is therefore needed to achieve the optimization of systems properties. In this concern, K. Kuorwel et al. (2013) considered the migration of carvacrol, thymol and linalool from starch-based films into a food simulant (Kuorwel et al., 2013), while L. Sánchez-González et al. (2011) studied the release of limonene present in chitosan films enriched with bergamot oil in food simulants (Sánchez-González et al., 2011). In another study, Tunc and Duma (2010) n tested the release of carvacrol from methyl cellulose/-montmorillonite nanocomposite (Tunç & Duman, 2010), whereas Nostro et al. (2012) investigated the effect of carvacrol and cinnamaldehydes from EVA copolymers (Nostro et al., 2012). Finally, some modelling work has also been considered to describe the release kinetics (Buonocore et al., 2003; Milovanovic et al., 2016). However, to the best of our knowledge, no values for diffusion coefficient of EOs have been obtained considering pure nanocellulose matrices (Ahankari et al., 2021b; Casalini & Baschetti, 2022). Some studies about the release of active compounds in food simulants could be found in the literature (Kashiri et al., 2017; Muriel-Galet et al., 2015; Souza et al., 2019), but these works are mainly related to the diffusion of the active agents in liquid media; very few information are instead available for the diffusion of essential oils in the vapor phase to mimic the evolution of the antimicrobial concentration in the headspace of an active packaging.

For these reasons, the focus of this study is the analysis of mass transport properties of Thyme, Cinnamon and Oregano EOs kept in direct contact with different types of nanocellulose, both considering the sorption from the liquid and the release of absorbed oils into the environment. These measurements can represent the first step to understand the release kinetic of this system, and to obtain information on the quantity of oils that can be embedded in such a matrix. They, are therefore of high importance to control and optimize the antimicrobial effect of the final active packaging solutions.

## 2. Materials and methods

### 2.1. Materials and film preparation

The Nanofibrillated Cellulose (NFC), obtained from bleached eucalyptus kraft pulp, was kindly provided by INOFIB as a water suspension. It was characterized by a negligible lignin content (in the order of 1%) and hemicellulose content of about 15%wt. Crystallinity of the material was close to 70%, in line with what usually observed for this system in literature. (Tonoli et al. 2016; Sanchez-Salvador et al. 2022). Pure NFC and surface modified carboxymethylated NFC (CMC-NFC, shown S.I. in figure A1) were used selecting three different types of materials: untreated NFC (indicated in the following as NFC1), CMC-NFC-780 (NFC2) and CMC-NFC-1600 (NFC3), which had, respectively, a final superficial charge density of *ca.* 30, 780 and 1600 μequiv/g. The CMC-NFC was synthetized by alkali-catalysed reaction of cellulose with monochloroacetic acid, as indicated in previous work, with a final diameter of 80–150 nm (Venturi et al., 2019) and a residual content of bigger fibers in the order of 10–15%.

Cinnamon, Thyme, and Oregano EOs were kindly provided by Destilerías Muñoz Gálvez, S.A. (Murcia, Spain). They were 100% pure oils, with respectively 74.7% v/v of *Eugenol,* 55.5% v/v of *Thymol* and 71.5% v/v of *Carvacrol.* The main properties of the different compounds present in the oils and the chemical structure of the major components are reported in SI. Both the nanocellulose and the essential oil have been used without any further purification, as this is the way they are often used in active packaging applications.

### 2.2. Nanocellulose films

Solvent casting technique was adopted to prepare a series of thin films for sorption and desorption tests. The NFC or CMC-NFC suspension was weighted with a standard laboratory balance. Then, distilled water was added until reaching the desired weight concentration (*ca.* 0.5–1.7 wt.%), which was chosen based on preliminary experiments. The solution was then homogenized with a high-speed homogenizer (IKA – T 18 digital ULTRA-TURRAX®), sonicated, and finally casted in a PTFE Petri dish of 9 cm of diameter, where it was left to dry at 35–40 °C for about 72 h. The thickness of the different samples, obtained through this protocol, was in the order of 30–50 μm, measured with a flat plate micrometer (Mitutoyo Absolute Series 227-221). In Table 1 it is possible to find the parameters used to create each sample, which were selected based on previous trials, done to understand the best conditions for the casting.

### 2.3. Sorption and desorption measurements

Several small pieces (about 10 mg in weight) were obtained from each cast film and put in vacuum conditions at 35 °C for 2 h, in order to remove all the water still present inside the matrix. After the weight and thickness of each piece were measured, they were put inside 20 ml glass vials. Each vial, containing one piece of nanocellulose, was filled with 2

**Table 1**
Nanocellulose casting parameters.

| Name | Material | Conc. (wt.%) | Homogenization (time and speed) | Drying Temperature (°C) |
|---|---|---|---|---|
| NFC1 | NFC | 0.50 | 10' x 10 k rpm | 35 |
| NFC2 | CMC-NFC-780 | 1.24 | 15' x 13 k rpm | 40 |
| NFC3 | CMC-NFC-1600 | 1.70 | 15' x 13 k rpm | 35 |

ml of Thyme or Oregano or Cinnamon essential oil. As a reference, one of the films was kept in the same conditions but without any essential oil. The samples were stored at ambient conditions and the weight was measured at fixed time intervals to monitor the absorption of the essential oil inside the polymer. Before each measurement, the sample was taken out from the vial and quickly dried with absorbing paper, until no trace of oil was detected on the paper. In this way, the excess of oil was removed from the surface of the nanocellulose. The balance used for experiments was an analytical balance Mettler Toledo AE 240 with a precision of $1 \times 10^{-4}$ g. The tests were performed at least in duplicate.

Desorption tests were performed at a temperature of 35 °C by using a Quartz Spring Microbalance (QSM) schematized in Fig. 1 and already described elsewhere (Piccinini et al., 2004). The spring had a sensitivity of 2 mm/mg and a maximum load of 100 mg. The sample was attached to the bottom of the spring and its weight variation was measured by monitoring the shortening of the spring, related to the EOs diffusing outside the membrane.

The experimentwas carried out by hanging a sample, previously equilibrated with the liquid essential oil in the 20 ml vial, to the spring and keeping it at atmospheric pressure and controlled temperature until the equilibrium conditions were reached, i.e. the column was saturated with the volatile compounds diffusing out from the sample. At that point, vacuum conditions were set inside the column, through the vacuum pump connected to the system, and the data were again collected until a new equilibrium was reached. At each step the final mass of the sample could be calculated following Eq. (1):

$$m_f = m_0 - (h_o - h_f)\cdot k/g \tag{1}$$

Where $k$ represents the spring elastic constant, $h_o$ and $h_f$ are the initial and final spring lengths and $g$ is the gravity acceleration. Since the experiment was carried out at ambient to vacuum pressure, the buoyancy force had been neglected. The resulting error was not affecting the results more than temperature oscillations and column leaks; the overall precision of the system, considering the noise of the measurements and the other uncertainties can be considered in the order of ± 5 μg.

The mass variations of the samples, due to the interactions with the EOs, in the adsorption and desorption tests were calculated as follows:

$$\frac{m_{ads}}{m_0} = \frac{(m_Q - m_0)}{m_0} \times 100 \tag{2}$$

$$\frac{m_{des}}{m_f} = \frac{(m_Q - m_f)}{m_f} \times 100 \tag{3}$$

Where $m_0$ is the initial mass of the sample, after being vacuumed and before being in contact with the oil; $m_Q$ is the mass of the sample after being immersed in the essential oil, prior the QSM measurement and $m_f$ is the final mass, after the QSM experiment and the final vacuum treatment. Theoretically, if no interactions and/or solubilization occur between the nanocellulose and the EOs, $m_f$ should be equal to $m_0$ within the experimental uncertainties. The latter are mainly related to the uncontrolled desorption of the EOs during sample handling, which cause weight losses in the order of 5%, as estimated by diffusivity data.

### 2.4. Diffusivity analysis

The information about weight change during time was used to investigate the EOs diffusion through the membrane. Different approaches can be used to fit the experimental data, by considering the different transport mechanisms of the penetrating molecules within the nanocellulose matrix.

If a purely diffusive mechanism is considered, and if the surfaces of the planar sample are kept at constant concentration during sorption, as in the case of liquid sorption experiments, Eq. 4 (Fick's model) can be used to estimate the diffusion coefficient, $D$ (Crank, 1975; Fieldson & Barbari, 1993).

$$\frac{m_t - m_0}{m_{inf} - m_0} = 1 - \sum_n \frac{8}{(2n+1)^2\pi^2} \exp\left[\frac{-D(2n+1)^2\pi^2 t}{L^2}\right] \tag{4}$$

Where $m_t$ is the mass of diffusing substance which has entered the sheet at time t, $m_{inf}$ is the same mass at the equilibrium condition and $L$ is the sample thickness. In the case of desorption in the gas phase, $m_t$ will be the mass of essential oil which left the membrane at time t. Eq. (4) can also be written in a different approximated form, valid for short time, where linear relationship can be obtained, simplifying the fitting procedures. Eq. (5) relates the mass uptake for short times (linear when reported against the square root of time):

$$\frac{m_t - m_0}{m_{inf} - m_0} = \frac{2}{L}\left(\frac{D}{\pi}\right)^{1/2} t^{1/2} \tag{5}$$

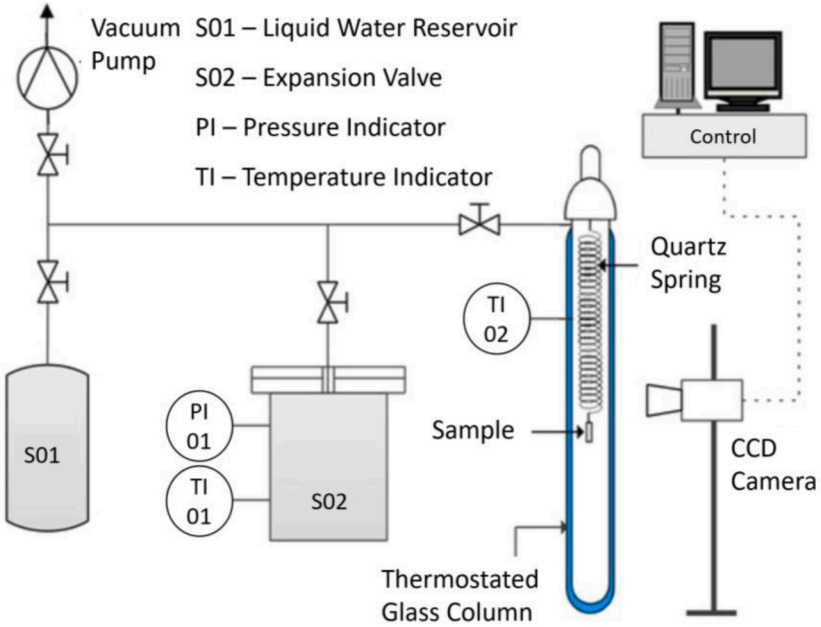


**Fig. 1.** Quartz spring apparatus set up (Venturi et al., 2019).

In the case of desorption experiments, instead, when the sample is suspended in a compartment of limited volume where the concentration of penetrant changes with time due to diffusion process, a different equation has to be used. If the external volume is well stirred, in particular, Eq. (6) can be used to estimate the diffusion coefficient, $D$ (Crank, 1975):

$$\frac{m_t - m_0}{m_{inf} - m_0} = 1 - \sum_{n=1}^{\infty} \frac{2\alpha(1+\alpha)}{1+\alpha+\alpha^2 q_n^2} \, exp\left(-\frac{Dq_n^2 t}{L^2}\right) \quad (6)$$

Where $m_t$ represents the mass of essential oil exiting the membrane at time t and $m_{inf}$ corresponds to the mass of the sample at the end of the tests, prior to the vacuum step needed to recover the initial weight. Also, $q_n$ are the non-zero positive roots of the equation $\tan q_n = -\alpha q_n$, with $\alpha$ representing the ratio of the volumes of solution and of the sheet rescaled with the partition coefficient, which was needed to account for the differences in the equilibrium concentration of solute within the surface of the sheet with respect to the solution.

The previous relationship holds when, as said above, the diffusion is Fickian. Therefore, the kinetics of the sorption or desorption process can be described by Eqs 4 – 6. However, more complex diffusion behaviours can be encountered. As an example, a second diffusion coefficient can be taken into consideration, by assuming that different species are diffusing contemporarily and independently in the sample, thus changing the Eq. (6) into Eq. (7) describing a Dual Fickian Sorption (DFS) process:

$$\frac{m_t - m_0}{m_{inf} - m_0} = 1 - (1-\beta)\sum_{n=1}^{\infty} \frac{2\alpha(1+\alpha)}{1+\alpha+\alpha^2 q_n^2} \, exp\left(-\frac{D_1 q_n^2 t}{l^2}\right) - \beta \sum_{n=1}^{\infty} \frac{2\alpha(1+\alpha)}{1+\alpha+\alpha^2 q_n^2} \, exp\left(-\frac{D_2 q_n^2 t}{l^2}\right) \quad (7)$$

Where the factor $\beta$ indicates the relative influence of the two diffusion coefficients on the process. In particular, the first diffusion coefficient ($D_1$) usually represents the diffusion at short times, while the latter ($D_2$) represents the diffusion at long times. $\beta$, therefore, represents the weight of the slow kinetics in the overall desorption process.

Another possibility is to consider a different modelling approach, such as the "Parallel exponential kinetics" (PEK), which has been already used to describe transport of water in nanocellulose (Belbekhouche et al., 2011) as well as in natural fibers such as lyocell, cotton (Okubayashi et al., 2004), flax, hemp and others (Kohler et al., 2003).

The model assumes two parallel independent first order processes that refer to different sorption/desorption sites. In the case of nanocellulose, it has been suggested to target the fast sorption sites in the amorphous region of the films. While the slow sorption sites were considered to be embedded in the crystalline parts of the sample (Belbekhouche et al., 2011). According to the PEK model, the mass sorption at time $t$ over the total mass absorbed at $t = inf$ is related to time as shon in Eq. (8):

$$\frac{m_t - m_0}{m_{inf} - m_0} = \varphi_{PEK}\left(1 - e^{-t/\tau_1^{PEK}}\right) + (1-\varphi_{PEK})\left(1 - e^{-t/\tau_2^{PEK}}\right) \quad (8)$$

Where $\varphi_{PEK}$ is a parameter which indicates the relative weight of each process in the overall sorption, $\tau$ is a characteristic time of the sorption process, and the subscripts 2 and 1 refer to the fast (small $\tau$) and the slow (high $\tau$) kinetic processes, respectively.

### 2.5. FTIR-ATR spectroscopy

IR analysis was carried out on the different films before and after the absorption of the EOs, to ensure the complete removal of the essential oil from the nanocellulose after the desorption and to check for possible interaction among the fibers and the oil which could lead to matrix modification.

An AVATAR 380 Infrared spectrometer (Nicolet, Thermo Fisher Scientific Inc.) provided with an Attenuated Total Reflection tool (MIRacle™, Pike Technologies) was used for the tests. The spectra were acquired by pressing the film at room conditions directly on the ZnSe ATR crystal, with a calibrated pressure in order to ensure repeatability of the results. Each acquisition employed 32 scans per spectrum with a resolution of 4 $cm^{-1}$. The samples were analysed before and after the sorption/desorption experiments, in order to see how the contact with the essential oil could impact the structure of the film. All analyses were performed at least in duplicate.

## 3. Results and discussion

### 3.1. Film characterization

In Fig. 2, the film obtained by casting NFC1 is shown as example. All the films from the different nanocellulose types have the same appearance, uniform and opaque, with a whiteish colour. They resulted brittle during the handling, especially after the vacuum step, which substantially reduced the amount of water within the samples.

Fig. 3 shows the IR analysis comparison of the different nanocellulose types. NFC1 refers to pure nanocellulose, while NFC2 and NFC3 refer to different carboxymethylation degrees, 780 μeq/mol and 1600 μeq/mol, respectively. The spectra are rather similar but with clear variations in the peaks, which can be related to the variation of the chemical structure going from the pure nanocellulose to the carboxymethylated one. For example, the broad absorption band at 3333 $cm^{-1}$, attributed to the stretching frequency of the –OH group, is more evident in the NFC1 and tends to decrease increasing the carboxymethylation degree, though it is not completely disappearing because of residual OH present in the system and because it is overlapping with the broad absorption band at 3307 $cm^{-1}$, due to the stretching frequency of the –COO– group (Mandal & Chakrabarty, 2019). The small peak detected around 1726 $cm^{-1}$, on the other hand, corresponds to the C=O stretching frequency of carboxylic acid groups and results to increase going from NFC1 to NFC3 (Chi & Catchmark, 2018). Same behaviour was found for the bands around 1400 $cm^{-1}$, assigned to the presence of O-H bending related to a carboxylic acid, which also increases with carboxymethylation degree, covering the bending vibration of the C-H and C-O groups of polysaccharide aromatic ring visible at 1300–1370 $cm^{-1}$ (Phanthong et al., 2016). The band at 1028 $cm^{-1}$, due to C–O asymmetric bridge stretching, seems shifted to lower wavenumber with the increase of the surface charge in the sample. Also, the band at 862 $cm^{-1}$, appearing for the carboxymethylated nanocellulose, is related to C-O-C stretching (Bicu & Mustata, 2011).

### 3.2. Absorption and desorption measurements

The comparison between the absorbed and the desorbed mass by different NFC types when immersed in the liquid EOs is shown in Fig. 4, as calculated from Eqs (2) and (3). In particular, equilibrium data at the end of the sorption were compared with data obtained by weighting each sample after the desorption of the essential oil in the QSM and after

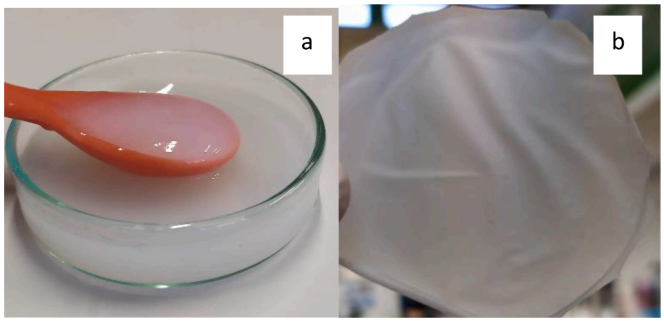


**Fig. 2.** Nanocellulose solution (NFC1) in water (a) and nanocellulose casted film (b).

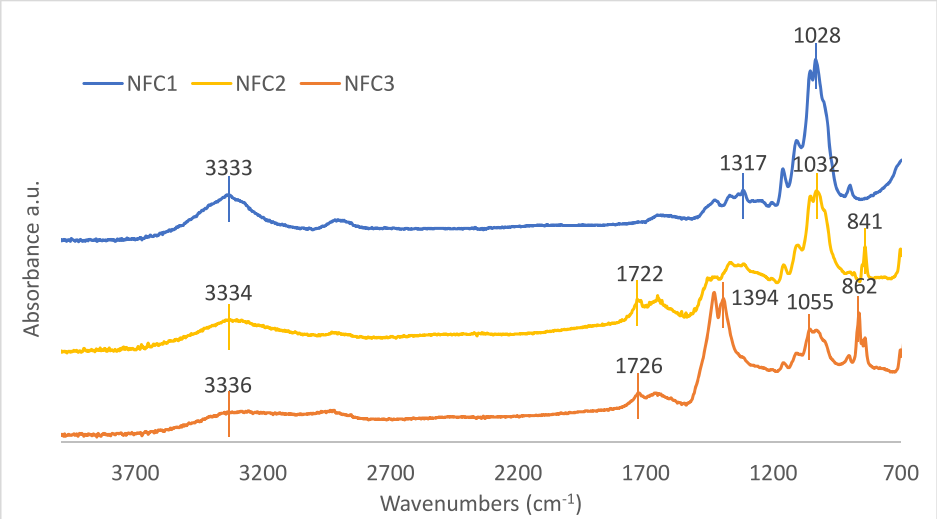


**Fig. 3.** FT-IR analysis of the three different types of nanocellulose. NFC1 refers to pure nanocellulose, while NFC2 and NFC3 refer to different carboxymethylation degrees, 780 μeq/mol and 1600 μeq/mol, respectively.

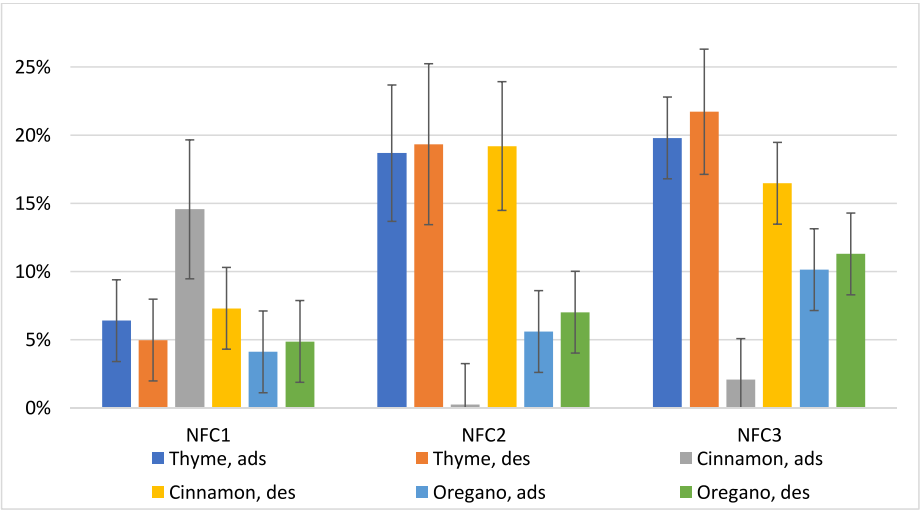


**Fig. 4.** Comparison between the absorbed and desorbed mass, considering the mass lost during the experiment set up. The data are presented for the three different oils and the three different nanocellulose types, as indicated in the legend.

an additional vacuum treatment was applied. All the tests were repeated at least twice and the values reported were obtained by averaging the different results.

It is possible to observe very different behaviours for the various oils and nanocellulose types, regarding the amount of oil absorbed and the difference between data obtained from sorption and desorption. Indeed, thyme and oregano results are substantially stable and consistent since the mass values obtained in the two tests are rather similar, within the uncertainty of the measurements. For cinnamon, on the other hand, the desorbed mass is substantially lower than the absorbed one in the case of NFC1, but definitely higher in NFC2 and NFC3, which actually showed final values of mass uptake very close to 0. The observed behaviour is likely due to a difficulty in completely remove the cinnamon from the pure nanocellulose at the end of the first experiment, and to a non-negligible solubilization of the carboxymethylated NFC during the sorption tests in the second and third cases, as it will be better discussed in the following section. For this reason, in the current analysis, only the desorption values observed for cinnamon will be considered for NFC2 and NFC3 as a measure of the total mass uptake in the sample. While for NFC1 the final value at the end of the sorption will be considered as the more consistent result.

Considering the oils solubility, it can be seen from Fig. 4 that thyme and oregano absorbed mass monotonously increases going from NFC1 to NFC3, with thyme showing the higher solubility, ranging from 5 to 20% wt. Oregano has solubility similar to thyme in NFC1, but results less affected by surface charge, reaching a value of only 10% for NFC3. Cinnamon behaviour is instead substantially different, with values of solubility in the three samples in the range of 15–20%, and therefore rather similar to each other, considering the uncertainty of the measurements.

The mass sorption as a function of the time for cinnamon, thyme and oregano EOs in NFC2 is reported in Fig. 5 a, b, and c respectively. The behaviour of the three oils in the NFC matrix is rather similar for short time, with a fast sorption up to a peak which, in case of thyme and cinnamon, is then followed by a decrease of the sorbed mass with time. However, while for thyme this desorption is rather limited, in time and mass loss, for cinnamon it continues also for long times, substantially reducing the absorbed mass at the end of experiments to values often very close to 0. This effect is likely due to a partial dissolution of the matrix, as also confirmed by the final mass of the sample measured after

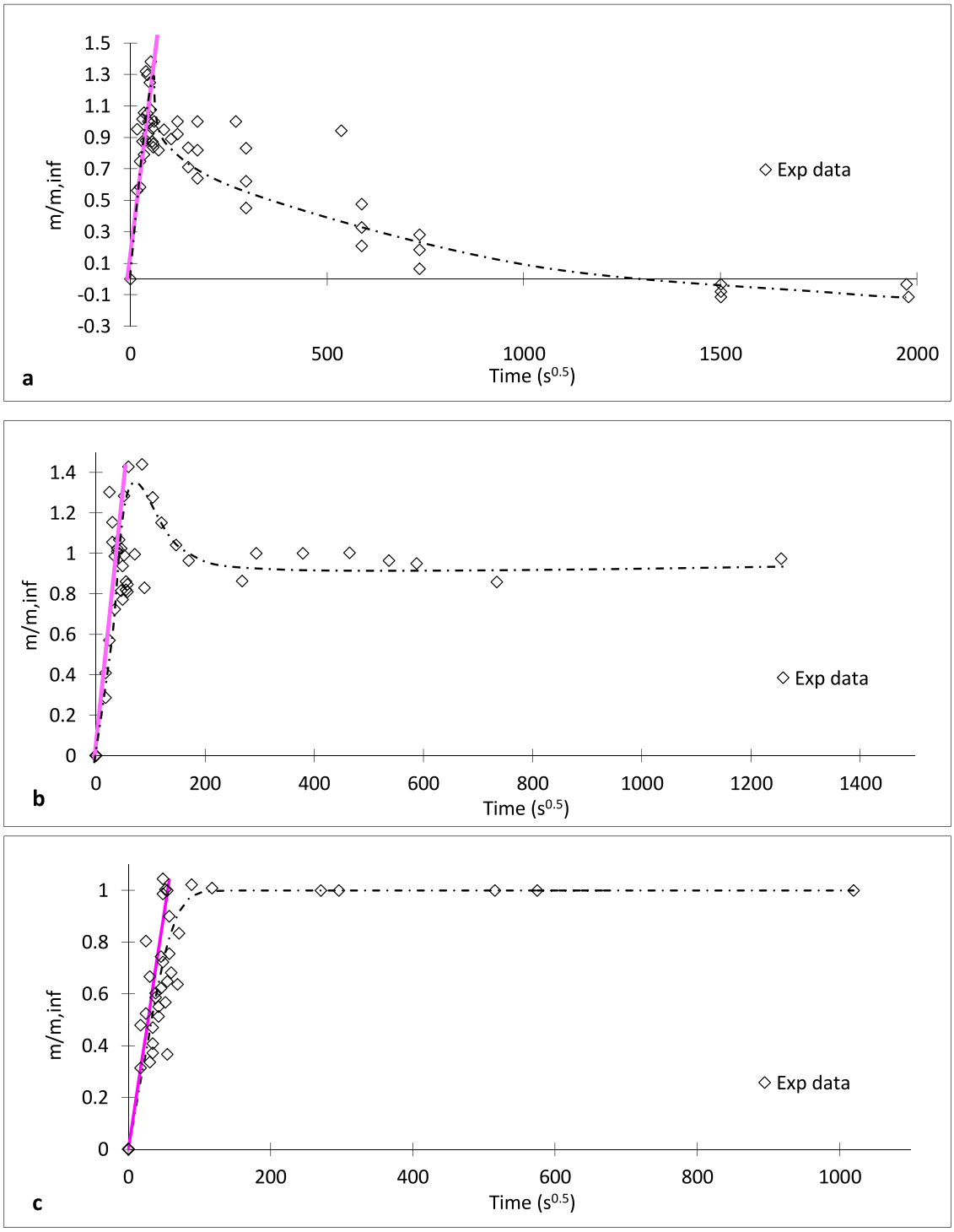


**Fig. 5.** Cinnamon (a), Thyme (b) and Oregano (c) essential oil absorption in NFC2.

completing the desorption tests (Fig. 4). Indeed, while for oregano and thyme differences in the order of 2–3% were measured, well inside the experimental uncertainty, for cinnamon in NFC2 and NFC3 values in the order of 13–16% were obtained, with the final mass always lower than the initial one.

The FTIR spectra of the different samples was repeated at the end of the sorption tests and after the final vacuum treatment. Fig. 6a compares the NFC2 prior and after being in contact with Cinnamon essential oil. Compared to the pure NFC spectrum (light blue line), the NFC immersed in the oil (orange line) also contains the small but clear characteristic peaks of the cinnamon essential oil (blue line). Absorption peaks are indeed observed around 1512 $cm^{-1}$ and 1265 $cm^{-1}$, which can be related, respectively, to the nitrogen compounds and the aromatic amine present in the oil (Montero et al., 2021; Syafiq et al., 2021b). Interestingly, however, other modifications are visible, which remain also after vacuum is applied (yellow line in Fig. 6a). The peak near 839 $cm^{-1}$ present in pure nanocellulose is indeed missing in the other spectra, as well as the ones around 1700 $cm^{-1}$, which seem to disappear upon cinnamon addition or somewhat shift at 1514 $cm^{-1}$, where a new peak is formed. All these modifications confirm the existence of strong and non-reversible oil-matrix interactions. As an example, the peak at 900 $cm^{-1}$ is often associated with the β-glycosidic linkages between glucose

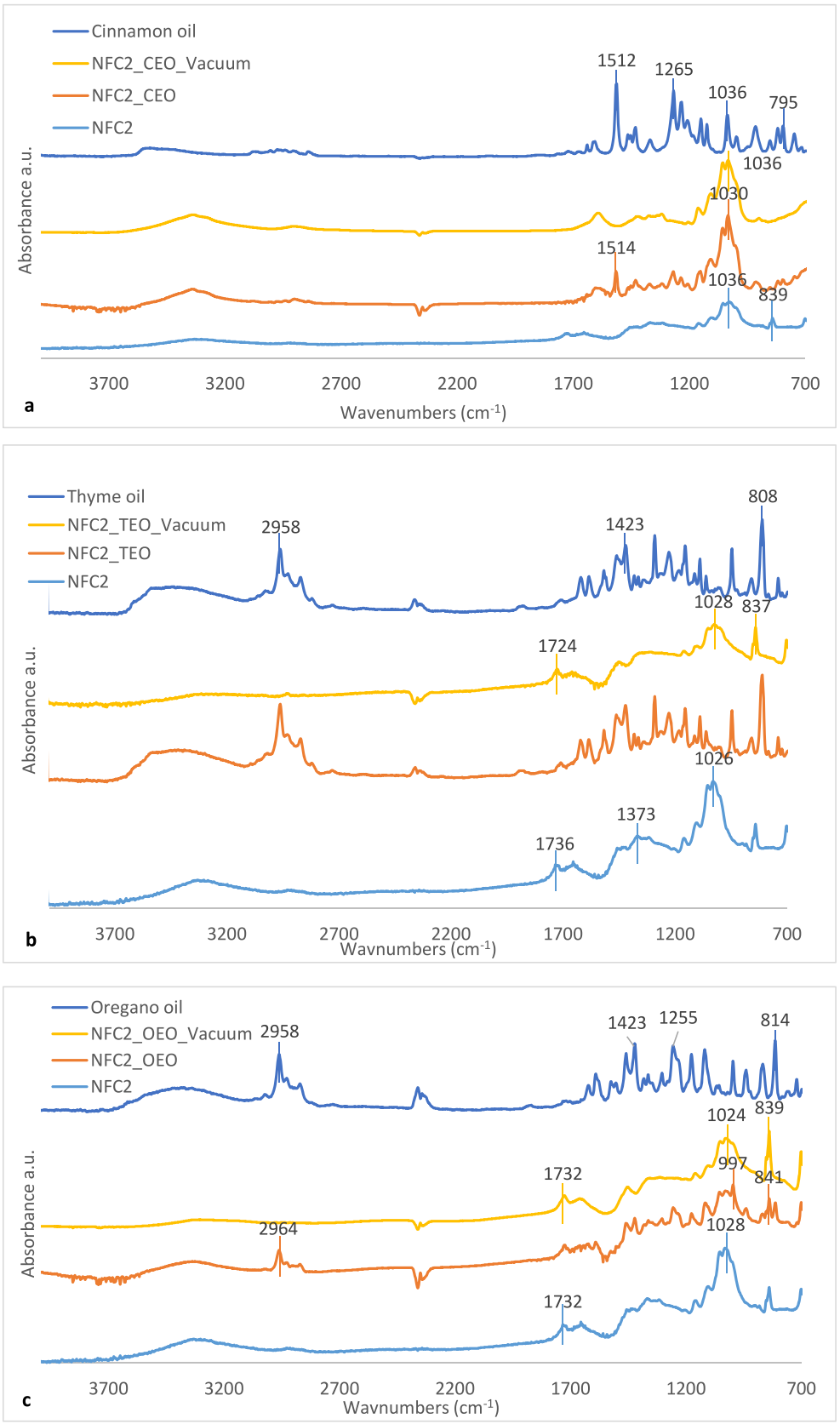


**Fig. 6.** FT-IR analysis of NFC2 prior and after being in contact with the cinnamon (a) thyme (b) and oregano (c) EOs. The spectra of pure oils have also been reported for comparison.

units in cellulose, which stands for cellulose II crystals. Its disappearance after the contact with the oil strengthens the hypothesis of strong interaction between nanocellulose and cinnamon essential oil (Carrillo et al., 2004; Mani Pujitha et al., 2017).

As a further confirmation, it is possible to observe Fig. 6b and c, which represent the IR spectra of NFC2 prior and after being in contact with thyme and oregano EOs, respectively. The NFC2 peaks remain substantially the same after the contact with the oil, even if with some differences, especially in the case of thyme, suggesting indeed the presence of some residue after the vacuum treatment. The spectra of the other types of nanocellulose with the cinnamon, thyme and oregano EOs can be observed in the S.I., and show a very similar behaviour with respect to cinnamon. Minor differences, instead, are observed for NFC1 which is the one that seems to better resist to solubilization. Being FTIR ATR a surface technique, it is not possible to use current data to estimate the possible loss of cellulosic materials during sorption. They, however, clearly indicate the existence of a strong interaction among cinnamon and carboxymethylated nanocellulose, which seems to cause more changes in the film structure with respect to other oils.

### 3.3. Diffusivity analysis

The absorption and desorption data are also used to perform a kinetics analysis of the oils transport inside the three different types of nanocellulose films.

Diffusivity values were obtained from sorption curves by hypothesizing a Fickian diffusion in line with the experimental evidence. From Fig. 5, despite the data scattering and the complex behaviour related to sample solubilization, it is quite evident that initial mass uptake is substantially linear with square root of time as obtained from Eq. 5. Therefore, the diffusivity was calculated through that equation, and the results are shown in Fig. 7. The chart clearly shows that for cinnamon and oregano the diffusion coefficient increases with the carboxymethylation degree of the film, while it is somewhat non monotonous in the case of thyme. In fact, for cinnamon the value of diffusivity for the pure nanocellulose films is in the order of $3.7 \times 10^{-9} cm^2/s$, increasing to $1.1 \times 10^{-8} cm^2/s$ for the carboxymethylated nanocellulose at 780 μeq/mol, and up to $2.0 \times 10^{-8} cm^2/s$ in the carboxymethylated nanocellulose at 1600 μeq/mol. Similar behaviour is observed for oregano that, however, has generally lower diffusivity, ranging from $1.0 \times 10^{-9}$ to $4.4 \times 10^{-9}\ cm^2/s$ in NFC1 and NFC3 respectively. Thyme, on the other hand, does not show a clear trend as NFC2 and NFC3 have the same diffusion coefficient, in the order of $7.6 \times 10^{-9}\ cm^2/s$, which remains in any case more than three times higher than the one of untreated nanocellulose.

The surface modification, therefore, seems to speed up the diffusion process as if the higher surface charge is able to increase the spacing between fibers, thus facilitating the transport of the different oils across the films. This hypothesis was also considered to explain the behaviour of water diffusion into pure and surface modified nanocellulose films (Ansaloni et al., 2017).

In general, then, cinnamon essential oil has the higher diffusion coefficient, followed by thyme and oregano. These effects can be associated with the interactions occurring between the essential oil and the nanocellulose and the ability of the former to relax the bonding within the cellulose chains. From this point of view, the high diffusivity of cinnamon can be easily related to its ability to cause major changes in the nanocellulose matrix up to a point where part of the chains results solubilized in the oil. Thyme solubility, on the other hand, is clearly higher than the oregano one in all the samples inspected. So that the higher diffusivity can be directly related to the higher swelling of the nanocellulose matrix. It is well known, indeed, that in dry conditions nanocellulose is a quite barrier material and relaxation of the interfibrillar bonding is needed to allow different vapor and gases to penetrate its structure (Minelli et al., 2010).

As made for the absorption, the kinetics of the desorption process was studied by considering the behaviour of the mass change as a function of time.

An example of the data obtained in this experiment is reported in Fig. 8 a and b which show, respectively, the thyme desorption from NFC1 and oregano desorption from NFC2. In the plots, the vertical axis which reports the normalized mass uptake, calculated through Eq. 9:

$$normalized\ mass\ uptake = \frac{m_t - m_0}{m_{inf} - m_0} \tag{9}$$

Data fitting was carried on with the different kinetic models previously described and it results that while DFS is more suited to describe thyme desorption, PEK results more adequate for catching the oregano behaviour.

In both cases, the data suggest that two different stages exist: a first

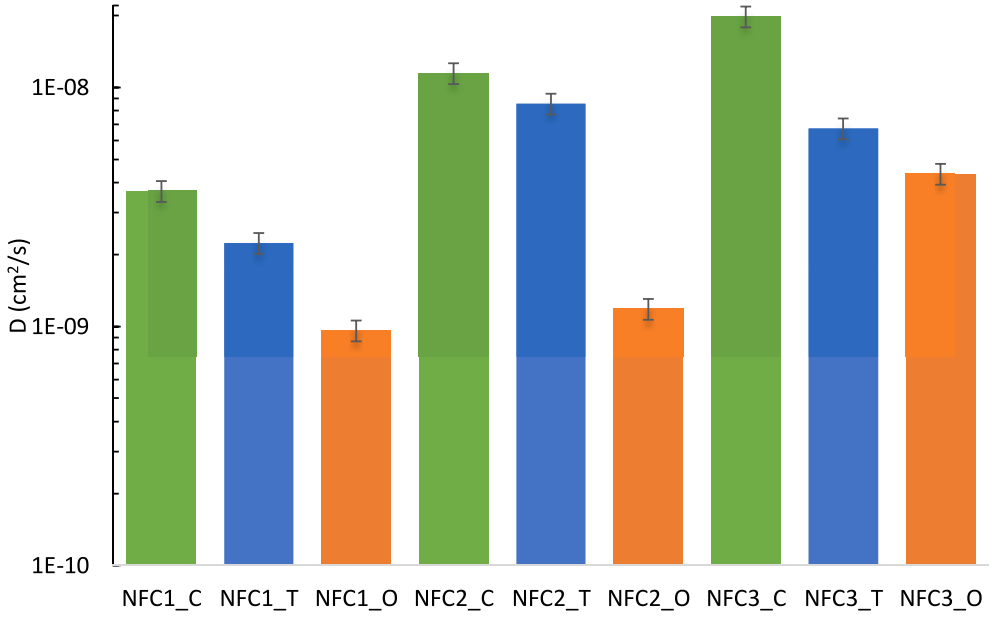


**Fig. 7.** Diffusion coefficient estimated from absorption in liquid phase for Cinnamon (green), Thyme (blue) and Oregano (orange) EOs in different nanocellulose matrices.

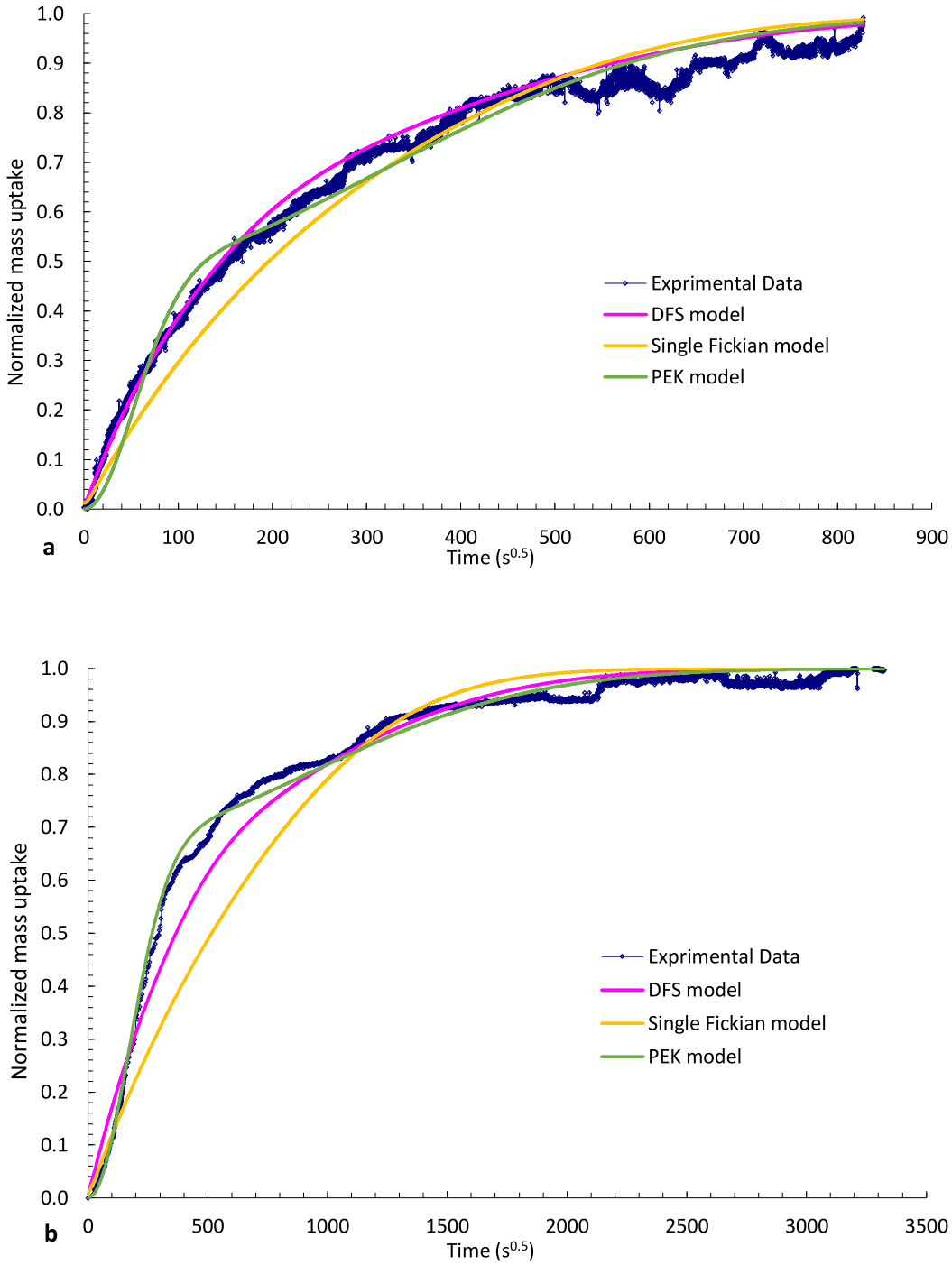


**Fig. 8.** Desorption kinetics of EOs from nanocellulose films: (a) thyme desorption from NFC1 (b) oregano desorption from NFC2.

one where the oils desorb at a high rate from the swollen matrix, followed by a second stage where, likely due to the lower amount of oil, the packing density of the fibers increases, and the desorption becomes more difficult.

The type of kinetics that better describes the data is not common to all the systems, making it difficult to draw general trends. An overview of the fitting results is given by Table 2, while charts of the data fitting for all the systems inspected are reported in the SI.

By analysing the data from tables, it is interesting to notice that both φ and β parameters are generally spanning in the range of 0.3–0.7, confirming that two processes are generally needed for the correct interpretation of the desorption behaviour. The only exception is represented by thyme-NFC3 desorption data, where $D_1$ and $D_2$ obtained from fitting of DSF model are substantially equivalent. For all the other systems, instead, φ and β values are well correlated as systems of high φ show high β and vice versa. In particular, among the different oils, oregano is the one with lower φ (and $\beta$), while cinnamon and thyme show very similar values. Oregano, therefore, is the oil for which the fast desorption has a higher importance with respect to the slow one. Interestingly it is also the oil for which PEK usually shows a better fit of the experimental data, as it can be seen from the last two columns of Table 2, which report the global and short time average relative error defined by Eq. 10:

$$err\%_{ave} = \sum_{n=1..N}\left[\left(\frac{\left|m_{model} - m_{expdata}\right|}{m_{exp\ data}}\right)_n \frac{1}{n}\right] \quad (10)$$

**Table 2**
PEK and DFS parameters for all the samples. The column MSE indicates the mean square error of the model compared to the experimental data.

| PEK model data | | | | | |
|---|---|---|---|---|---|
| Sample | τ1 | τ2 | ϕPEK | % Relative error (total) | % Relative error (short time) |
| NFC1_C | $5.0 \times 10^5$ | $3.6 \times 10^3$ | 0.49 | 5% | 11% |
| NFC1_T | $2.0 \times 10^5$ | $5.3 \times 10^3$ | 0.52 | 10% | 22% |
| NFC1_O | $4.0 \times 10^4$ | $1.2 \times 10^3$ | 0.22 | 2% | 16% |
| NFC2_C | $6.0 \times 10^4$ | $1.7 \times 10^3$ | 0.60 | 3% | 28% |
| NFC2_T | $3.8 \times 10^4$ | $1.4 \times 10^3$ | 0.55 | 3% | 8% |
| NFC2_O | $1.7 \times 10^6$ | $5.6 \times 10^4$ | 0.33 | 3% | 29% |
| NFC3_C | $2.6 \times 10^5$ | $1.6 \times 10^4$ | 0.50 | 4% | 32% |
| NFC3_T | $6.4 \times 10^4$ | $2.0 \times 10^3$ | 0.70 | 9% | 18% |
| NFC3_O | $5.2 \times 10^4$ | $1.7 \times 10^3$ | 0.25 | 1% | 7% |
| DFS model data | | | | | |
| Sample | D1 | D2 | β | % Relative error (total) | % Relative error (short time) |
| NFC1_C | $3.85 \times 10^{-11}$ | $3.80 \times 10^{-13}$ | 0.68 | 5% | 40% |
| NFC1_T | $2.50 \times 10^{-11}$ | $2.20 \times 10^{-12}$ | 0.67 | 6% | 13% |
| NFC1_O | $1.10 \times 10^{-9}$ | $4.00 \times 10^{-11}$ | 0.30 | 2% | 38% |
| NFC2_C | $1.00 \times 10^{-9}$ | $2.90 \times 10^{-11}$ | 0.73 | 2% | 20% |
| NFC2_T | $6.60 \times 10^{-11}$ | $1.10 \times 10^{-11}$ | 0.67 | 3% | 39% |
| NFC2_O | $1.17 \times 10^{-11}$ | $1.20 \times 10^{-12}$ | 0.57 | 4% | 48% |
| NFC3_C | $2.50 \times 10^{-10}$ | $1.50 \times 10^{-11}$ | 0.70 | 3% | 9% |
| NFC3_T | $9.94 \times 10^{-12}$ | $9.97 \times 10^{-12}$ | 0.23 | 7% | 12% |
| NFC3_O | $4.22 \times 10^{-10}$ | $3.50 \times 10^{-11}$ | 0.33 | 4% | 55% |

Where N represents, respectively, the total number of data points for the total error, and the short time data points for short time errors. Short time indicates here the time interval needed for the desorbed mass to reach the amount assigned by the given model (PEK or DSF) to the fast process (proportional to 1-φ and 1-β respectively).

This latter error was introduced as the total errors are usually dominated by long time data and could not properly describe the initial stage of the desorption, where the main differences between the two models are encountered.

From the table it can be seen, indeed, that the obtained total errors are generally low and comparable for the two models, since long time data are generally described fairly well by both PEK and DFS approach. Short time errors, on the other hand, show well defined differences reflecting the Fickian (as in Fig. 8a) rather than the exponential kinetics of the data (clearly visible from Fig. 8b).

Therefore, oregano short time data, results in general well described by an exponential behaviour, with errors for PEK never exceeding 30% against those observed for DFS which are spanning between 38 and 55%. For the other oils the situation is less clear; both cinnamon and thyme data, indeed, are mainly Fickian, even if short time exponential behaviour was dominant in some of the films considered, namely NFC2 for thyme and NFC1 for cinnamon.

The present data are in line with other literature results, both in terms of diffusivity values and transport behaviour. In the first case, in the absence of specific studies about the thyme, oregano and cinnamon diffusion in nanocellulose, some information, can be found considering the transport of these essential oils or of their main constituents (such as Eugenol, Carvacrol and Thymol as reported in Table 1 in S.I.) in other matrices, to have at least a confirmation of the diffusivity values observed. In this concern, Muriel-Galet et al. studied the release of oregano essential oil from ethylene vinyl alcohol copolymer films, obtaining a diffusion coefficient in the order of $10^{-11}$ $cm^2/s$ (Muriel-Galet et al., 2015). While in another work Kashiri et al., (2017) studied the release of thymol and carvacrol, from zein films incorporated with Zataria multiflora Boiss. Essential oil and found diffusivity values at 37 °C in the range of 4 and 5 x $10^{-11}$ $cm^2/s$ for the two oils respectively. More in general different studies analyze the diffusivity of active components present in the various essential oils and the results generally span in the range $10^{-8}$–$10^{-11}$ $cm^2/s$ depending on the matrix itself and on other parameters such as the temperature and the humidity. (Mascheroni et al., 2011; Ramos et al., 2014; Wu et al., 2018)

Considering instead the complex transport behaviour observed during EOs release, this is confirmed by several studies involving both polymers and fibers. Mishra et al. (2018), for example, studied the retention of lemongrass essential oil loaded on cellulose nanofibre-polyethylene glycol composite. The results suggested that Fickian diffusion makes the predominant contribution to release of major aroma compounds (Mishra et al., 2018). Also, release studies conducted on ethylcellulose-encapsulated thyme essential oil showed a time-dependent Fickian diffusion (González-Reza et al., 2020). Instead, J. Ke et al. (2019) studied the diffusion kinetics of cinnamaldehyde from corn starch-based film into food simulant. The compound followed a Fickian behaviour with relevant differences between short and long times (Ke et al., 2019). Another interesting work was done by Montero et al. (2021) on polybutylene adipate-co-terephthalate films added with nanocellulose and functionalized with cinnamon essential oil (Montero et al., 2021). Here, as well, a pseudo Fickian diffusion was observed, with a faster release at short times, maybe due to the non-adsorbed oil on the nanocellulose surface, which quickly migrates on the polymer surface thus causing a burst effect at the beginning of the experiment. In addition to such results, the diffusion kinetics in microfibrillated cellulose is known to strongly depend on film swelling. As an example, non Fickian sorption behaviour was observed in many different types of nanocellulose, when equilibrated with water vapor at high relative humidity (Belbekhouche et al., 2011; Meriçer et al., 2017; Minelli et al., 2010). In fact, the water causes the swelling of the matrix, which leads to a relaxation of the chains of the polymer and a consequent change in the diffusion mechanism (Rosa et al., 2001).

In this concern the strong interaction of the EOs with the nanocellulosic matrix is confirmed by desorption data analysis which also suggests, following Montero et al. (Montero et al., 2021), that the higher fraction of mass desorbed in short time in case of oregano can be related a lower ability of this oil to bind with the cellulose matrix.

Another consideration could be made by comparing absorption and desorption kinetics. Even with the limitation of the fitting approach, it clearly results that the diffusion coefficients calculated during sorption from liquid phase are definitely higher (usually 1 order of magnitude) with respect to the D1 values obtained for short time desorption rates. Therefore, the transport of the different oils in the nanocellulose seems to be dominated by the relaxation and swelling of the fibrous matrix, higher in the liquid rather than in the gas phase, while other sources of complexity play a secondary role, such as, for example, the effects related to EOs compositions. As already discussed, indeed, EOs are composed by a wide variety of compounds, which strongly differ in both molecular weight and volatility (boiling point or vapor pressure) and that are expected to have different diffusion behaviour.

In this concern, a detailed study of the gas leaving the film would be useful, in order to have a better description of the overall system behaviour, but this was not possible with the present experimental set up. The kinetics analysis, however, suggests that, in view of the foreseen application, the quantity of oils present in the matrix can guarantee an antimicrobial activity even at long times. Indeed, based on φ and β values and on the concentration, molecular weight and the vapor pressure of the EOs' components (Table A1 in the SI), the most active compounds should be released in both desorption stages. In addition to that, for a complete analysis of the system antimicrobial activity, both on bacterial strains and on fresh packed food should be considered focusing

on the EOs effect in the vapor phase. This would allow indeed to avoid direct contact between the food and the essential oils thus reducing the alteration on the food taste which is often caused by the presence of the essential oils.

## 4. Conclusion

In this work, the absorption and diffusion of cinnamon, thyme and oregano EOs in nanocellulose films with increasing carboxymethylation degree were investigated in view of active packaging application. Indeed, sorption from the liquid phase was followed by desorption in the gas phase in a closed system trying to mimic the condition existing in fresh food packages.

The results showed that the absorption and desorption of the oils in these matrices depend on the carboxymethylation degree and on the oil types. In particular, thyme essential oil showed the highest solubility with values of mass uptake close to 20%wt. for the nanocellulose with a surface charge of 1600 μeq/mol, against a value of only 10%wt in the case of oregano, which resulted the oil with lower solubility.

The kinetics of the sorption process resulted substantially Fickian, allowing the determination of diffusivity values in the order of $10^{-8} - 10^{-9}\ cm^2/s$. The trend was generally increasing with the carboxymethylation degree. Cinnamon essential oil had the highest diffusivity, followed by thyme and oregano, suggesting that affinity with the nanocellulose and the ability to swell its structure were the main factors affecting the kinetics of the sorption. For the release in the gas phase two different kinetics were needed to satisfactorily describe the experimental data, which showed a fast release at short times followed by a slower process at long time. Interestingly, while thyme and cinnamon data could be well described by considering a two separate Fickian processes, oregano release was better fitted by considering a parallel exponential kinetics. Despite their difference, however, both approaches were consistent in determining the relative weight of the fast and slow kinetics.

This preliminary study confirms that the absorption and release of EOs from nanocellulose matrices can be controlled by adequately choosing the type of nanocellulose. It also suggests that the analysis of mass transport of different active substances in the nanocellulose matrix can give useful information and useful guidelines in the development of new bio-active food packaging solutions. In fact, on the base of such information it would be possible to tune the essential oil concentration within the matrix and to obtain the desired release rate over time, in order to extend the duration of the antimicrobial and antioxidant activity.

## Author statement

Sara Casalini: Writing – Original draft, Writing, Investigation, Visualization, Validation

Federico Montanari: Investigation, Visualization

Marco Giacinti Baschetti: Data Curation, Validation, Review & Editing, Supervision

## Declaration of Competing Interest

The authors declare that they have no known competing financial interests or personal relationships that could have appeared to influence the work reported in this paper.

## Data Availability

Data will be made available on request.

## Supplementary materials

Supplementary material associated with this article can be found, in the online version, at doi:10.1016/j.carpta.2022.100271.

## References


Agarwal, S. (2020). Biodegradable polymers: Present opportunities and challenges in providing a microplastic-free environment. *Macromolecular Chemistry and Physics, 221*(6), Article 2000017. https://doi.org/10.1002/macp.202000017

Ahankari, S. S., Subhedar, A. R., Bhadauria, S. S., & Dufresne, A. (2021a). Nanocellulose in food packaging: A review. *Carbohydrate Polymers, 255*, Article 117479. https://doi.org/10.1016/j.carbpol.2020.117479

Ahankari, S. S., Subhedar, A. R., Bhadauria, S. S., & Dufresne, A. (2021b). Nanocellulose in food packaging: A review. *Carbohydrate Polymers, 255*, Article 117479. https://doi.org/10.1016/J.CARBPOL.2020.117479

Ansaloni, L., Salas-Gay, J., Ligi, S., & Baschetti, M. G. (2017). Nanocellulose-based membranes for CO2 capture. *Journal of Membrane Science, 522*, 216–225. https://doi.org/10.1016/j.memsci.2016.09.024

Atarés, L., & Chiralt, A. (2016). Essential oils as additives in biodegradable films and coatings for active food packaging. *Trends in Food Science and Technology, 48*, 51–62. https://doi.org/10.1016/j.tifs.2015.12.001

Azeredo, H. M. C., Rosa, M. F., & Mattoso, L. H. C. (2017). Nanocellulose in bio-based food packaging applications. *Industrial Crops and Products, 97*, 664–671. https://doi.org/10.1016/j.indcrop.2016.03.013

Belbekhouche, S., Bras, J., Siqueira, G., Chappey, C., Lebrun, L., Khelifi, B., Marais, S., & Dufresne, A. (2011). Water sorption behavior and gas barrier properties of cellulose whiskers and microfibrils films. *Carbohydrate Polymers, 83*(4), 1740–1748. https://doi.org/10.1016/j.carbpol.2010.10.036

Bicu, I., & Mustata, F. (2011). Cellulose extraction from orange peel using sulfite digestion reagents. *Bioresource Technology, 102*(21), 10013–10019. https://doi.org/10.1016/J.BIORTECH.2011.08.041

Bras, J., & Saini, S. (2017). Nanocellulose in functional packaging. *Cellulose-reinforced nanofibre composites: Production, properties and applications* (pp. 175–213). https://doi.org/10.1016/B978-0-08-100957-4.00008-5

Buonocore, G. G., Del Nobile, M. A., Panizza, A., Corbo, M. R., & Nicolais, L. (2003). A general approach to describe the antimicrobial agent release from highly swellable films intended for food packaging applications. *Journal of Controlled Release, 90*(1), 97–107. https://doi.org/10.1016/S0168-3659(03)00154-8

Burt, S. (2004). Essential oils: Their antibacterial properties and potential applications in foods - a review. *International Journal of Food Microbiology, 94*(3), 223–253. https://doi.org/10.1016/j.ijfoodmicro.2004.03.022

Carrillo, F., Colom, X., Suñol, J. J., & Saurina, J. (2004). Structural FTIR analysis and thermal characterisation of lyocell and viscose-type fibres. *European Polymer Journal, 40*(9), 2229–2234. https://doi.org/10.1016/J.EURPOLYMJ.2004.05.003

Casalini, S., & Baschetti, M. G. (2022). The use of essential oils in chitosan or cellulose-based materials for the production of active food packaging solutions: A review. *Journal of the Science of Food and Agriculture*. https://doi.org/10.1002/JSFA.11918

Chi, K., & Catchmark, J. M. (2018). Improved eco-friendly barrier materials based on crystalline nanocellulose/chitosan/carboxymethyl cellulose polyelectrolyte complexes. *Food Hydrocolloids, 80*, 195–205. https://doi.org/10.1016/j.foodhyd.2018.02.003

Crank, J. (1975). The mathematics of diffusion. *Physics Bulletin, 26*, 500.

Dannenberg, G., da, S., Funck, G. D., Cruxen, C. E., dos, S., Marques, J.de L., Silva, W. P. da, & Fiorentini, Â. M. (2017). Essential oil from pink pepper as an antimicrobial component in cellulose acetate film: Potential for application as active packaging for sliced cheese. *LWT - Food Science and Technology, 81*, 314–318. https://doi.org/10.1016/j.lwt.2017.04.002

Ferrer, A., Pal, L., & Hubbe, M. (2017). Nanocellulose in packaging: Advances in barrier layer technologies. *Industrial Crops and Products, 95*, 574–582. https://doi.org/10.1016/j.indcrop.2016.11.012

Fieldson, G. T., & Barbari, T. A. (1993). The use of FTi.r.-a.t.r. spectroscopy to characterize penetrant diffusion in polymers. *Polymer, 34*(6), 1146–1153. https://doi.org/10.1016/0032-3861(93)90765-3

García, A., Gandini, A., Labidi, J., Belgacem, N., & Bras, J. (2016). Industrial and crop wastes: A new source for nanocellulose biorefinery. *Industrial Crops and Products, 93*, 26–38. https://doi.org/10.1016/j.indcrop.2016.06.004

González-Reza, R. M., Hernández-Sánchez, H., Zambrano-Zaragoza, M. L., Gutiérrez-López, G. F., Del-Real, A., Quintanar-Guerrero, D., & Velasco-Bejarano, B. (2020). Influence of stabilizing and encapsulating polymers on antioxidant capacity, stability, and kinetic release of thyme essential oil nanocapsules. *Foods 2020, 9*(12), 1884. https://doi.org/10.3390/FOODS9121884, 9, 1884.

Habibi, Y. (2014). Key advances in the chemical modification of nanocelluloses. *Chemical Society Reviews, 43*, 1519–1542. https://doi.org/10.1039/c3cs60204d

Hammer, K. A., Carson, C. F., & Riley, T. V. (1999a). Antimicrobial activity of essential oils and other plant extracts. *Journal of Applied Microbiology, 86*(6), 985–990. https://doi.org/10.1046/j.1365-2672.1999.00780.x

Hammer, K. A., Carson, C. F., & Riley, T. V. (1999b). Antimicrobial activity of essential oils and other plant extracts. *Journal of Applied Microbiology, 86*(6), 985–990. https://doi.org/10.1046/j.1365-2672.1999.00780.x

Ibrahim, Nabil A., Eid, Basma M., & Sharaf, Samar (2020). Nanocellulose: Extraction, surface functionalization and potential applications. In Vijay Kumar Thakur, Ellisabet Frollini, & Janet Scott (Eds.), *Cellulose nanoparticles: Chemistry and fundamentals*. Royal Society of Chemistry Publisher. vol. 1, 2021. pp. 149-177.

Kashiri, M., Cerisuelo, J. P., Domínguez, I., López-Carballo, G., Muriel-Gallet, V., Gavara, R., & Hernández-Muñoz, P. (2017). Zein films and coatings as carriers and release systems of Zataria multiflora Boiss. Essential oil for antimicrobial food packaging. *Food Hydrocolloids, 70*, 260–268. https://doi.org/10.1016/J.FOODHYD.2017.02.021

Ke, J., Xiao, L., Yu, G., Wu, H., Shen, G., & Zhang, Z. (2019). The study of diffusion kinetics of cinnamaldehyde from corn starch-based film into food simulant and physical properties of antibacterial polymer film. *International Journal of Biological Macromolecules, 125*, 642–650. https://doi.org/10.1016/j.ijbiomac.2018.12.094

Khaledian, Y., Pajohi-Alamoti, M., & Bazargani-Gilani, B. (2019). Development of cellulose nanofibers coating incorporated with ginger essential oil and citric acid to extend the shelf life of ready-to-cook barbecue chicken. *Journal of Food Processing and Preservation*, (10), 43. https://doi.org/10.1111/jfpp.14114

Khalil, Abdul, S, H. P., Davoudpour, Y., Islam, M. N., Mustapha, A., Sudesh, K., Dungani, R., & Jawaid, M (2014). Production and modification of nanofibrillated cellulose using various mechanical processes: A review. *Carbohydrate Polymers, 99*, 649–665. https://doi.org/10.1016/j.carbpol.2013.08.069

Khan, A., Huq, T., Khan, R. A., Riedl, B., & Lacroix, M. (2014a). Nanocellulose-based composites and bioactive agents for food packaging. *Critical Reviews in Food Science and Nutrition, 54*(2), 163–174. https://doi.org/10.1080/10408398.2011.578765

Khan, A., Huq, T., Khan, R. A., Riedl, B., & Lacroix, M. (2014b). Nanocellulose-based composites and bioactive agents for food packaging. *Critical Reviews in Food Science and Nutrition, 54*(2), 163–174. https://doi.org/10.1080/10408398.2011.578765

Klemm, D., Cranston, E. D., Fischer, D., Gama, M., Kedzior, S. A., Kralisch, D., Kramer, F., Kondo, T., Lindström, T., Nietzsche, S., Petzold-Welcke, K., & Rauchfuß, F. (2018). Nanocellulose as a natural source for groundbreaking applications in materials science: Today's state. *Materials Today, 21*(7), 720–748. https://doi.org/10.1016/j.mattod.2018.02.001

Kohler, R., Dück, R., Ausperger, B., & Alex, R. (2003). A numeric model for the kinetics of water vapor sorption on cellulosic reinforcement fibers. *Composite Interfaces, 10*(2–3), 255–276. https://doi.org/10.1163/156855403765826900

Kuorwel, K. K., Cran, M. J., Sonneveld, K., Miltz, J., & Bigger, S. W. (2013). Migration of antimicrobial agents from starch-based films into a food simulant. *LWT - Food Science and Technology, 50*(2), 432–438. https://doi.org/10.1016/j.lwt.2012.08.023

Li, F., Mascheroni, E., & Piergiovanni, L. (2015). The potential of nanocellulose in the packaging field: A review. *Packaging Technology and Science, 28*(6), 475–508. https://doi.org/10.1002/pts.2121

Mandal, A., & Chakrabarty, D. (2019). Studies on mechanical, thermal, and barrier properties of carboxymethyl cellulose film highly filled with nanocellulose. *Journal of Thermoplastic Composite Materials, 32*(7), 995–1014.

Mani Pujitha, I., Khandelwal, M., Shekhar Sharma -, C., Monroe Keck, D., Islam, M., Martinez-Duarte, R., Yang, Y. P., Zhang, Y., Lang, Y. X., & Yu, M. H. (2017). Structural ATR-IR analysis of cellulose fibers prepared from a NaOH complex aqueous solution. *IOP Conference Series: Materials Science and Engineering*, 213(1), 012039. https://doi.org/10.1088/1757-899X/213/1/012039.

Mascheroni, E., Guillard, V., Gastaldi, E., Gontard, N., & Chalier, P. (2011). Anti-microbial effectiveness of relative humidity-controlled carvacrol release from wheat gluten/montmorillonite coated papers. *Food Control, 22*, 1582–1591.

Meriçer, Ç., Minelli, M., Giacinti Baschetti, M., & Lindström, T. (2017). Water sorption in microfibrillated cellulose (MFC): The effect of temperature and pretreatment. *Carbohydrate Polymers, 174*, 1201–1212. https://doi.org/10.1016/J.CARBPOL.2017.07.023

Milovanovic, S., Markovic, D., Aksentijevic, K., Stojanovic, D. B., Ivanovic, J., & Zizovic, I. (2016). Application of cellulose acetate for controlled release of thymol. *Carbohydrate Polymers, 147*, 344–353. https://doi.org/10.1016/j.carbpol.2016.03.093

Minelli, M., Baschetti, M. G., Doghieri, F., Ankerfors, M., Lindström, T., Siró, I., & Plackett, D. (2010). Investigation of mass transport properties of microfibrillated cellulose (MFC) films. *Journal of Membrane Science, 358*(1–2), 67–75. https://doi.org/10.1016/J.MEMSCI.2010.04.030

Mishra, D., Khare, P., Singh, D. K., Luqman, S., Kumar, Ajaya, P, V., Yadav, A., Das, T., & Saikia, B. K (2018). Retention of antibacterial and antioxidant properties of lemongrass oil loaded on cellulose nanofibre-poly ethylene glycol composite. *Industrial Crops and Products, 114*, 68–80. https://doi.org/10.1016/J.INDCROP.2018.01.077

Missoum, K., Belgacem, M. N., & Bras, J. (2013). Nanofibrillated cellulose surface modification: A review. *Materials, 6*(5), 1745–1766. https://doi.org/10.3390/ma6051745

Montero, Y., Souza, A. G., Oliveira, É. R., Rosa, D., & dos, S. (2021). Nanocellulose functionalized with cinnamon essential oil: A potential application in active biodegradable packaging for strawberry. *Sustainable Materials and Technologies, 29*, e00289. https://doi.org/10.1016/j.susmat.2021.e00289

Muriel-Galet, V., Cran, M. J., Bigger, S. W., Hernández-Muñoz, P., & Gavara, R. (2015). Antioxidant and antimicrobial properties of ethylene vinyl alcohol copolymer films based on the release of oregano essential oil and green tea extract components. *Journal of Food Engineering, 149*, 9–16. https://doi.org/10.1016/J.JFOODENG.2014.10.007

Nagarajan, K. J., Ramanujam, N. R., Sanjay, M. R., Siengchin, S., Surya Rajan, B., Sathick Basha, K., Madhu, P., & Raghav, G. R. (2021). A comprehensive review on cellulose nanocrystals and cellulose nanofibers: Pretreatment, preparation, and characterization. *Polymer Composites, 42*(4), 1588–1630. https://doi.org/10.1002/PC.25929

Nostro, A., Scaffaro, R., D'Arrigo, M., Botta, L., Filocamo, A., Marino, A., & Bisignano, G. (2012). Study on carvacrol and cinnamaldehyde polymeric films: Mechanical properties, release kinetics and antibacterial and antibiofilm activities. *Applied Microbiology and Biotechnology, 96*(4), 1029–1038. https://doi.org/10.1007/s00253-012-4091-3

Okubayashi, S., Griesser, U. J., & Bechtold, T. (2004). A kinetic study of moisture sorption and desorption on lyocell fibers. *Carbohydrate Polymers, 58*(3), 293–299. https://doi.org/10.1016/j.carbpol.2004.07.004

Othman, S. H. (2014). Bio-nanocomposite materials for food packaging applications: Types of biopolymer and nano-sized filler. *Agriculture and Agricultural Science Procedia, 2*, 296–303. https://doi.org/10.1016/j.aaspro.2014.11.042

Phanthong, P., Guan, G., Ma, Y., Hao, X., & Abudula, A. (2016). Effect of ball milling on the production of nanocellulose using mild acid hydrolysis method. *Journal of the Taiwan Institute of Chemical Engineers, 60*, 617–622. https://doi.org/10.1016/J.JTICE.2015.11.001

Piccinini, E., Giacinti Baschetti, M., & Sarti, G. C. (2004). Use of an automated spring balance for the simultaneous measurement of sorption and swelling in polymeric films. *Journal of Membrane Science, 234*(1–2), 95–100. https://doi.org/10.1016/j.memsci.2003.12.024

Pradhan, D., Jaiswal, A. K., & Jaiswal, S. (2022). Emerging technologies for the production of nanocellulose from lignocellulosic biomass. *Carbohydrate Polymers, 285*, Article 119258. https://doi.org/10.1016/J.CARBPOL.2022.119258

Qing, Y., Sabo, R., Zhu, J. Y., Agarwal, U., Cai, Z., & Wu, Y. (2013). A comparative study of cellulose nanofibrils disintegrated via multiple processing approaches. *Carbohydrate Polymers, 97*(1), 226–234. https://doi.org/10.1016/j.carbpol.2013.04.086

Ramos, M., Beltrán, A., Peltzer, M., Valente, A. J. M., & Garrigós, M.d. C. (2014). Release and antioxidant activity of carvacrol and thymol from polypropylene active packaging films LWT. - *Food Science and Technology, 58*(2), 470–477.

Reshmy, R., Philip, E., Thomas, D., Madhavan, A., Sindhu, R., Binod, P., Varjani, S., Awasthi, M. K., & Pandey, A. (2021). Bacterial nanocellulose: engineering, production, and applications. *Bioengineered, 12*(2), 11463. https://doi.org/10.1080/21655979.2021.2009753

Ribeiro-Santos, R., Andrade, M., de Melo, N. R., Santos, dos, F, R., Neves, I.de A., de Carvalho, M. G., & Sanches-Silva, A (2017). Biological activities and major components determination in essential oils intended for a biodegradable food packaging. *Industrial Crops and Products, 97*, 201–210. https://doi.org/10.1016/j.indcrop.2016.12.006

Ribeiro-Santos, R., Andrade, M., Melo, N. R.de, & Sanches-Silva, A (2017). Use of essential oils in active food packaging: Recent advances and future trends. *Trends in Food Science and Technology, 61*, 132–140. https://doi.org/10.1016/j.tifs.2016.11.021

Rol, F., Belgacem, M. N., Gandini, A., & Bras, J. (2019). Recent advances in surface-modified cellulose nanofibrils. *Progress in Polymer Science, 88*, 241–264. https://doi.org/10.1016/j.progpolymsci.2018.09.002

Rosa, F., Bordado, J., & Casquilho, M. (2001). Kinetics of water absorbency in AA/AMPS copolymers: Applications of a diffusion-relaxation model. *Polymer, 43*(1), 63–70. https://doi.org/10.1016/S0032-3861(01)00596-1

Salmieri, S., Islam, F., Khan, R. A., Hossain, F. M., Ibrahim, H. M. M., Miao, C., Hamad, W. Y., & Lacroix, M. (2014). Antimicrobial nanocomposite films made of poly(lactic acid)–cellulose nanocrystals (PLA–CNC) in food applications—Part B: Effect of oregano essential oil release on the inactivation of Listeria monocytogenes in mixed vegetables. *Cellulose, 21*, 4271–4285. https://doi.org/10.1007/s10570-014-0406-0

Sánchez-González, L., Cháfer, M., González-Martínez, C., Chiralt, A., & Desobry, S. (2011). Study of the release of limonene present in chitosan films enriched with bergamot oil in food simulants. *Journal of Food Engineering, 105*(1), 138–143. https://doi.org/10.1016/j.jfoodeng.2011.02.016

Sanchez-Salvador, J. L., Campano, C., Balea, A., Tarrés, Q., Delgado-Aguilar, M., Mutjé, P., Blanco, A., & Negro, C. (2022). Critical comparison of the properties of cellulose nanofibers produced from softwood and hardwood through enzymatic, chemical and mechanical processes. *International Journal of Biological Macromolecules, 205*, 220–230.

Shojaeiarani, J., Bajwa, D. S., & Chanda, S. (2021). Cellulose nanocrystal based composites: A review. *Composites Part C: Open Access, 5*, Article 100164. https://doi.org/10.1016/J.JCOMC.2021.100164

Silvestre, C., Duraccio, D., & Cimmino, S. (2011). Food packaging based on polymer nanomaterials. *Progress in Polymer Science (Oxford), 36*(12), 1766–1782. https://doi.org/10.1016/j.progpolymsci.2011.02.003

Souza, V. G. L., Rodrigues, C., Ferreira, L., Pires, J. R. A., Duarte, M. P., Coelhoso, I., & Fernando, A. L. (2019). In vitro bioactivity of novel chitosan bionanocomposites incorporated with different essential oils. *Industrial Crops and Products, 140*, Article 111563. https://doi.org/10.1016/J.INDCROP.2019.111563

Syafiq, R., Sapuan, S. M., & Zuhri, M. R. M. (2021a). Antimicrobial activity, physical, mechanical and barrier properties of sugar palm based nanocellulose/starch biocomposite films incorporated with cinnamon essential oil. *Journal of Materials Research and Technology, 11*, 144–157. https://doi.org/10.1016/J.JMRT.2020.12.091

Syafiq, R., Sapuan, S. M., & Zuhri, M. R. M. (2021b). Antimicrobial activity, physical, mechanical and barrier properties of sugar palm based nanocellulose/starch biocomposite films incorporated with cinnamon essential oil. *Journal of Materials Research and Technology, 11*, 144–157. https://doi.org/10.1016/j.jmrt.2020.12.091

Tonoli, G. H. D., Holtman, K. M., Glenn, G., et al. (2016). Properties of cellulose micro/nanofibers obtained from eucalyptus pulp fiber treated with anaerobic digestate and high shear mixing. *Cellulose, 23*, 1239–1256. https://doi.org/10.1007/s10570-016-0890-5

Tunç, S., & Duman, O. (2010). Preparation and characterization of biodegradable methyl cellulose/montmorillonite nanocomposite films. *Applied Clay Science, 48*(3), 414–424. https://doi.org/10.1016/J.CLAY.2010.01.016

Venturi, D., Chrysanthou, A., Dhuiège, B., Missoum, K., & Giacinti Baschetti, M. (2019). Arginine/nanocellulose membranes for carbon capture applications. *Nanomaterials, 9*(6), 877. https://doi.org/10.3390/nano9060877

Vilarinho, F., Sanches Silva, A., Vaz, M. F., & Farinha, J. P. (2018). Nanocellulose in green food packaging. *Critical Reviews in Food Science and Nutrition, 58*(9), 1526–1537. https://doi.org/10.1080/10408398.2016.1270254

Wikström, F., Verghese, K., Auras, R., Olsson, A., Williams, H., Wever, R., Grönman, K., Kvalvåg Pettersen, M., Møller, H., & Soukka, R. (2019). Packaging strategies that save food: A research agenda for 2030. *Journal of Industrial Ecology, 23*(3), 532–540. https://doi.org/10.1111/jiec.12769

Wróblewska-Krepsztul, J., Rydzkowski, T., Borowski, G., Szczypiński, M., Klepka, T., & Thakur, V. K. (2018). Recent progress in biodegradable polymers and nanocomposite-based packaging materials for sustainable environment. *International Journal of Polymer Analysis and Characterization, 23*(4), 383–395. https://doi.org/10.1080/1023666X.2018.1455382

Wu, Y. M., Wang, Z. W., C Ying, Hu, & Nerin, C (2018). Influence of factors on release of antimicrobials from antimicrobial packaging materials. *Critical Reviews in Food Science and Nutrition, 58*(7), 1108–1121.

Yildirim, S., Röcker, B., Pettersen, M. K., Nilsen-Nygaard, J., Ayhan, Z., Rutkaite, R., Radusin, T., Suminska, P., Marcos, B., & Coma, V. (2018). Active packaging applications for food. *Comprehensive Reviews in Food Science and Food Safety, 17*(1), 165–199. https://doi.org/10.1111/1541-4337.12322

Yousefi, H., Su, H. M., Imani, S. M., Alkhaldi, K., Filipe, C. D., & Didar, T. F. (2019). Intelligent food packaging: A review of smart sensing technologies for monitoring food quality. *ACS Sensors, 4*(4), 808–821. https://doi.org/10.1021/acssensors.9b00440

Youssef, A. M., & El-Sayed, S. M. (2018). Bionanocomposites materials for food packaging applications: Concepts and future outlook. *Carbohydrate Polymers, 193*, 19–27. https://doi.org/10.1016/j.carbpol.2018.03.088

Zhao, X., Cornish, K., & Vodovotz, Y. (2020). Narrowing the gap for bioplastic use in food packaging: An update. *Environmental Science & Technology, 54*(8), 4712–4732. https://doi.org/10.1021/acs.est.9b03755